Polymer Testing 94 (2021) 107042

Contents lists available at ScienceDirect

Polymer Testing

journal homepage: http://www.elsevier.com/locate/polytest

Near infrared to ultraviolet upconversion nanocomposite for controlling the permittivity of polyspiropyran shell

Xiaotao Wang [a,**], Xiaoping Liu [a], Hongda Zhu [a], Gaowen Zhang [a], Xuefeng Li [a,***], Chak-Yin Tang [b,*], Wing-Cheung Law [b], Xin Zhao [c]

[a] Hubei Provincial Key Laboratory of Green Materials for Light Industry, Collaborative Innovation Center for Green Light-weight Materials and Processing, School of Materials Science and Engineering, Hubei University of Technology, Wuhan, Hubei Province, 430068, PR China
[b] Department of Industrial and Systems Engineering, The Hong Kong Polytechnic University, Hung Hom, Kowloon, Hong Kong SAR, PR China
[c] Department of Biomedical Engineering, The Hong Kong Polytechnic University, Hung Hom, Kowloon, Hong Kong SAR, PR China

ARTICLE INFO

Keywords:
Up-conversion nanoparticle
Dual-responsive
Controlled drug release
Nanocomposite

ABSTRACT

Near infrared to ultraviolet (NIR-to-UV) up-conversion nanocomposites, composed of an upconversion nanoparticle (UCNP) core and a transformable polyspiropyran shell, were prepared by distillation precipitation polymerization and the template method. The polyspiropyran shell can undergo reversible hydrophobic-hydrophilic transformations through the switching of UV and visible light and by variation of pH. About 10 wt% of the anticancer drug, doxorubicin (DOX), can be loaded into the drug carrying layer under pH 7.4 by electrostatic force. The NIR and pH responsive features of the polyspiropyran shell were shown by the dynamic light scattering (DLS) results, in which the size of nanocomposites (UCNPs@SP-MA/MAA) became larger under NIR irradiation and pH 4.5. The hydrophobic to hydrophilic surface transformation alters the permittivity of the polyspiropyran shell and the release behavior. The cumulative release rate of the DOX-loaded UCNPs@SP-MA/MAA reached 53.8% under pH 4.5 and NIR irradiation. The cytotoxicity of the bare UCNPs@SP-MA/MAA and the DOX-loaded UCNPs@SP-MA/MAA were evaluated against breast cancer cells and the results confirmed that the toxicity of UCNPs@SP-MA/MAA nanocomposites was minimal, even at high dosage (100 μg/mL), while the toxicity of DOX can be triggered by NIR light.

1. Introduction

Application of responsive polymers has become an important research topic because it is one of the enabling technologies for fabricating controlled drug-release devices that can have stimuli-responsive properties at a particular time and space [1–4]. In various internal or external stimuli (pH, photo, thermal, ionization) [5–8], light is more favorable due to its flexibility in regards to adjustable wavelength and irradiation time, and its capability as a remote trigger. The idea of photo-responsive polymers is typically realized by introducing photosensitive moieties into polymers that can have physical or chemical changes by light irradiation. One of the common designs is diblock copolymer that contains hydrophilic and hydrophobic groups, connecting by photosensitive groups to shift the hydrophilic/hydrophobic balance [9–13]. Another strategy is photoisomerization. Photo-isomers, such as azobenzene [14,15], spiropyran [16], diarylethene [17,18] and stilbene [19,20], have been incorporated with inorganic nanostructures to confer drug carrying and controlled release abilities. Among them, spiropyran [16] has its uniqueness in the reversible structural transformations between hydrophobic spiropyran (SP) and hydrophilic merocyanine (MC), accompanying with ring-opening, under different external stimuli, such as light, metal ions, pH, redox potential, mechanical force and temperature [21,22].

Self-assembly of spiropyranyl polymer is one of the most used methods to synthesize micelles or nanocarriers. The drug release can be realized by changing the stability of the micelle and the dissociation under the irradiation of UV light. Zhao [23] and co-workers developed several payload-released models and achieved drug release of spiropyran and PLGA20-b-PEO460 by shifting the hydrophilic−hydrophobic balance. Wang's group [24] synthesized a

* Corresponding author.
** Corresponding author.
*** Corresponding author.
E-mail addresses: xiaotaowang@hbut.edu.cn (X. Wang), li_xf@mail.hbut.edu.cn (X. Li), cy.tang@polyu.edu.hk (C.-Y. Tang).

https://doi.org/10.1016/j.polymertesting.2020.107042
Received 20 August 2020; Received in revised form 15 December 2020; Accepted 23 December 2020
Available online 28 December 2020

light-controlled reversible double-layered spiropyran block copolymer membrane. Upon UV irradiation, controlled release of 2′-deoxy-5--fluorouridine (5-dFu) was achieved through the permeable transformation from hydrophobicity to hydrophilicity. Chen's team [25] designed a spiropyran-based amphiphilic random copolymer and light-, pH-, and thermally multi-responsive micellar nanoparticle by the self-assembly method for biological applications. Kotharangannagari [26] synthesized a light-responsive micellar constructed of spiropyran and PLGA20-b-PEO460 block copolymer. After UV exposure, the flower-like micelle was broken in an aqueous solution. However, low-intensity UV light cannot penetrate into the lesions whereas high-power UV could be harmful to the human body.

Recently, rare earth doped up-conversion nanoparticles (UCNPs) have been widely used due to their unique energy level structures, which can absorb multiple low-energy (long-wavelength) photons (e.g. NIR) and up-convert the energy to UV and visible light [27–34]. In addition, an NIR laser (700–1100 nm) can penetrate deeper into human skin without damaging the tissue [35,36]. UCNPs can serve as the bridge between the UV-responsive polymer and low-energy NIR light [37,38]. Liu's group designed a cage structure for grafted spiropyran molecules on the surface of UCNPs [39]. The particle surface became unstable due to the change of spiropyran polarity, resulting in drug release under the NIR stimulation. Chen [40] and co-workers constructed a micelle through the self-assembly method with the encapsulation of UCNPs and induced the isomerization of hydrophobic spiropyran (SP) to merocyanine (MC), which ruptured the spherical structure. Nevertheless, *in vivo* stability is also a critical factor for the self-assembly of UCNP-polymer structures.

Our group has focused on constructing robust monodispersed photo-responsive nanocomposites [41]. In our previous work, a multi-layered nanocomposite structure was composed of inorganic UCNP as the core and a silica layer as the template accompanied by coating with a transformable spiropyran layer. After the silica layer was dissolved, the inner layer UCNPs in the yolk could convert the NIR light to UV that can be absorbed by the spiropyran. The variation of hydrophilicity of the nanocomposites can be used to control the encapsulation and release of drugs. Furthermore, pH responsive as an endogenic stimulus, with the hydrophilic (MC/MCH+)- hydrophobic (SP) changes, would also trigger the intracellular drug release.

2. Experimental

2.1. Materials and methods

Y_2O_3, Yb_2O_3, and Tm_2O_3 (≥99.0%) were from Yuelong New Material Co., Shanghai, China. Analytical grade oleic acid (OA; 90%, TCI), 1-octadecene (ODE; 95%, Aladdin), hydroquinone (≥99.0%, Aladdin), sodium hydroxide (≥98%, Aladdin), and ammonium fluoride (NH_4F, 98%, Aladdin) were supplied by Aladdin Reagent Co., Ltd., Shanghai, China. Acetonitrile, cyclohexane, tetraethyl orthosilicate (TEOS), and ammonia aqueous (28 wt%) were obtained from Beijing Chemicals Reagents, China. Deionized water was used in all experiments. YCl_3, $YbCl_3$, and $TmCl_3$ were synthesized by Y_2O_3, Yb_2O_3, and Tm_2O_3, respectively. All other reagents were analytically grade and used without further purification.

2.2. Preparation of $NaYF_4$: Yb^{3+}/Tm^{3+} up-conversion nanoparticles

An aqueous solution of YCl_3 (0.8 mmol), $YbCl_3$ (0.2 mmol), and $TmCl_3$ (5 μmol) ions were stirred in a 100 mL flask which was placed on a heating mantle. Then 7 mL of oleic acid and 15 mL of 1-octadecene were added and stirred in a nitrogen atmosphere. The flask was slowly heated to 110 °C and then connected to a vacuum pump to remove extra water and oxygen. When there was no bubbles in the flask, the temperature was raised to 140 °C and maintained for 50 min. After cooling down to room temperature, 5 mL of NaOH-methanol (2.5 mmol) solution and 8 mL of NH_4F-methanol (4.1 mmol) solution were added into a 15 mL centrifuge tube and ultrasonically mixed for 60 min. The temperature of flask was then raised to 45 °C for 30 min to start preliminary nucleation, followed by raising the temperature to 70 °C to evaporate the methanol. When the solution in the flask became yellow and uniformly stable, it was heated to 300 °C and maintained for 90 min under nitrogen, then cooling down to room temperature. Finally, the prepared $NaYF_4$: Yb^{3+}/Tm^{3+} nanoparticles were purified by centrifugation at 12,000 rpm for 30 min and washed several times with ethanol/cyclohexane and stored in 8 mL chloroform.

2.3. Preparation of $NaYF_4$: Yb^{3+}/Tm^{3+}@$NaYF_4$ core–shell UCNPs

Similarly, $NaYF_4$:Yb^{3+}/Tm^{3+}@$NaYF_4$ nanoparticles (UCNPs) were prepared using the Ostwald ripening method as described above. The prepared $NaYF_4$:Yb^{3+}/Tm^{3+} nanoparticles were placed in a 100 mL flask, then 1 mmol aqueous solution of YCl_3 was added. To remove water and oxygen, 7 mL of oleic acid and 15 mL of 1-octadecene were added dropwise followed by heating the flask to 110 °C and keeping it at 110 °C for 20 min under a nitrogen atmosphere until there were no bubbles in the bottle. The mixture was heated to 140 °C for 50 min until the solution turned yellow, and was then naturally cooled down to room temperature. 3.5 mL of NaOH-methanol solution and 2 mL of NH_4F-methanol solution were premixed by ultrasonic treatment at room temperature. The mixture was then quickly added to the reaction flask and stirred at room temperature for 1 h. For nucleation, the temperature was increased to 45 °C for 30 min. After removing the methanol and chloroform by raising the temperature to 70 C, the reaction solution was rapidly heated to 300 °C and maintained at 140 °C for 90 min. The nanoparticles were collected by centrifugation and washed with methanol to remove some residual oleic acid and redispersed in 10 mL of cyclohexane.

2.4. Synthesis of $NaYF_4$:Yb^{3+}/Tm^{3+}@$NaYF_4$@SiO_2 nanoparticles

The core–shell $NaYF_4$: Yb^{3+}/Tm^{3+}@$NaYF_4$@SiO_2 nanoparticles were prepared via a reverse microemulsion method by using $NaYF_4$: Yb^{3+}/Tm^{3+}@$NaYF_4$ core-shell particles prepared as above precursors with CO-520 as surfactant and cyclohexane as solvent. In this method, 1.3 mL of CO-520, 20 mL of cyclohexane and 0.9 mL of 0.1 mol UCNPs were mixed by ultrasonic treatment for 0.5 h to obtain a uniform suspension. Next, 0.16 mL of NH_4F (30 wt%) was added to the mixed solution, and then ultrasonically treated for 30 min. After that, 250 μL of tetraethyl orthosilicate (TEOS) was added dropwise to the solution, and the mixture was stirred at 550 rpm for 24 h. To modify the surface of the microspheres and improve the hydrophilicity of the UCNPs@SiO_2 nanoparticle surface, 2.5 mL of methacryloxy propyl trimethoxyl silane (MPS) was added to the dispersion and stirred at the same rate for a further 24 h. The obtained UCNPs@SiO_2 nanoparticles were centrifuged at 1200 r/min for 45 min, washed four times with 1.5 mL of acetone and 3 mL of ethanol, and then the precipitate was dried in a vacuum.

2.5. Synthesis of 1′-(2-methacryloxyethyl)-3′,3′- dimethyl-6-nitrospiro-(2H-1 benzopyran- 2,2′- indoline) monomer (SP-MA)

The 1′-(2-methacryloxyethyl)-3′,3′-dimethyl-6-nitrospiro-(2H-1benzopyran-2,2 -indoline) monomer (SP-MA) was synthesized according to Ref. [42]. The SP-MA was prepared by a dehydration reaction. Specifically, 350 mg of dicyclohexylcarbodiimide (DCC), 80 mL of dichloromethane and 1.06 mL of methacrylic acid were added one-by-one to a 100 mL three-necked flask, and the flask was placed in a water bath and stirred for 10 min under a nitrogen atmosphere. Then, 417 mg (1.19 mmol) spiropyran and a catalytic amount of 4-dimethylaminopyridine (DMAP) were added to the flask. To ensure a complete reaction, the solution was stirred in the dark at ambient temperature for two days. The organic solution was washed with hydrochloric acid (10%),

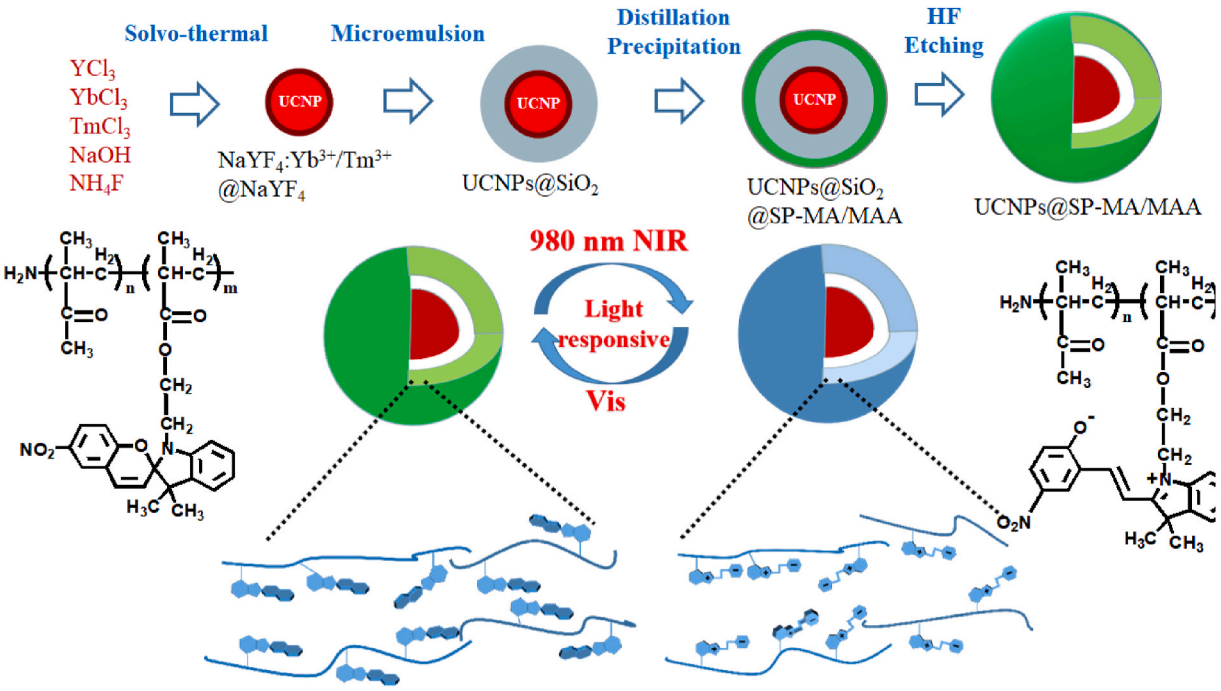

Scheme 1. Schematic diagram showing the synthesis of UCNPs@SP-MA/MAA nanocomposites.

followed by saturated Na_2CO_3, and deionized water. Anhydrous magnesium sulphate was added to remove excess water for 24 h. The solvent was evaporated and the crude material was crystalized from ethyl acetate.

2.6. Synthesis of UCNPs@SiO_2@SP-MA/MAA

UCNPs@SiO_2@SP-MA/MAA nanoparticles were prepared by distillation precipitation polymerization. 30 mg of vinylated UCNPs@SiO_2 nanospheres was added to a flask containing 160 mL of acetonitrile and was uniformly dispersed in acetonitrile by sonication for 30 min. This was followed by the addition of a mixture of SP-MA (0.7905 g), ethyleneglycol dimethacrylate (EGDMA, 78 μL, 25% n (SP-MA)), MAA (10 μL, 15% n (SP-MA)), pre-purified AIBN (0.0226 g, 2 wt% relative to comonomer) that was added to the flask equipped with a water-oil separator, condenser, receiver and nitrogen protection. The flask was immersed in a heating mantle and the reaction mixture was heated from ambient temperature to 80 °C in 30 min and kept at 80 °C. After 80 mL of acetonitrile was distilled off from the reaction system within 4 h, the reaction was terminated by adding a small amount of a polymerization inhibitor Quinol. The resulting UCNPs@SiO_2@SP-MA/MAA nanoparticles were stored after centrifugation four times at 14,000 rpm for 50 min and re-dispersing in ethanol and *N*,*N*-Dimethylformamide (DMF), respectively.

2.7. Synthesis of dual-responsive nanocomposite (UCNPs@SP-MA/MAA)

To obtain a large drug-loading space, the UCNPs@SiO_2@SP-MA/MAA particles were dispersed in hydrofluoric acid (HF) and ethanol mixed solution for 48 h to remove the SiO_2 layer in the UCNPs@SiO_2@SP-MA/MAA nanospheres. Finally, the UCNPs@SP-MA/MAA was obtained. The excess HF and SiF_4 were expelled from the SP-MA/MAA nanospheres by centrifugation-redispersion cycles in methanol three times and dried for preservation.

2.8. Loading of doxorubicin (DOX)

UCNPs@SP-MA/MAA (20 mg) was added to 10 mL of deionized water (10 mg of DOX), and the solution was stirred at room temperature in a dark environment for 24 h. The DOX-UCNPs@SP-MA/MAA was separated from the drug solution by centrifugation at 14,000 rpm. Precipitates were washed three times with ethanol to completely remove the free DOX molecules adsorbed on the outer surface. The loading capacity of DOX on UCNPs@SP-MA/MAA nanocomposites was determined by fluorescent spectroscopic analysis at a wavelength of 480 nm, which was calculated by the difference in DOX concentration between the original DOX solution and the supernatant after loading.

2.9. Photo-triggered release behavior of DOX-UCNPs@SP-MA/MAA

The DOX-UCNPs@SP-MA/MAA nanocomposites (8 mg) were first dispersed in 1 mL deionized water, and the mixture was then transferred into the dialysis tubes with a molecular-weight cut off of 8000–14,000. The dialysis tubes were placed into reservoirs with 4 mL of water under NIR irradiation. The solution (3 mL) was periodically taken out to measure the absorption peak of DOX at 480 nm wavelength outside the dialysis tube, and then the test solution was quickly poured back into the container.

2.10. pH-triggered release behavior of DOX-UCNPs@SP-MA/MAA

DOX-UCNPs@SP-MA/MAA nanocomposites (8 mg) were dispersed in 1 mL of deionized water, and the mixture was subsequently transferred into a dialysis bag with 8000–14,000 kDa molecule weight cut-off. The dialysis tube was placed into a reservoir with 4 mL aqueous solutions at pH 4.5 and pH 7.4, respectively. After a certain time, the solution (3 mL) was taken out to measure the absorption peak intensity at 480 nm outside the dialysis bag and further calculate the concentration of DOX released.

2.11. In vitro cell viability assay

Cell viability studies of UCNPs@SP-MA/MAA and DOX-UCNPs@SP-

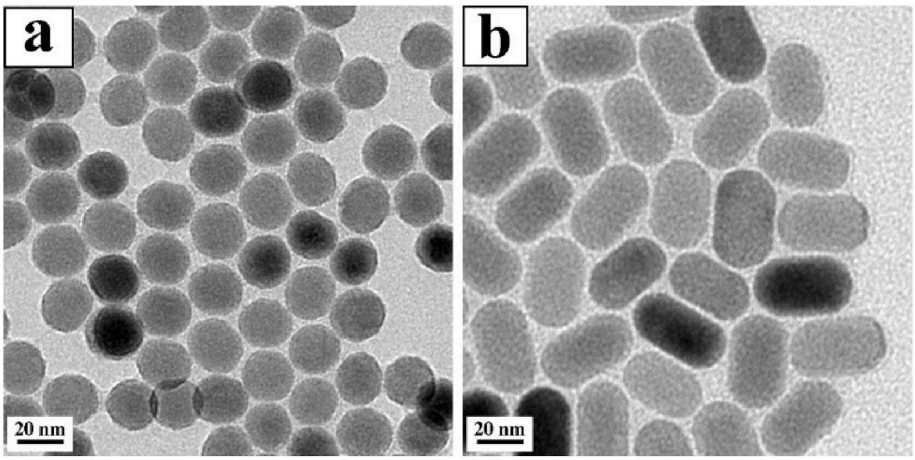

Fig. 1. TEM images of (a) $NaYF_4$: Yb^{3+}/Tm^{3+}, and (b) $NaYF_4$: Yb^{3+}/Tm^{3+}@$NaYF_4$.

MA/MAA were conducted using a standard 3-(4,5-dimethylthiazol-2-yl)-2,5-diphenyltetrazolium bromide (MTT) assay. MCF-7 was selected as the experimental cell line. MCF-7 cells with a density of 1×10^4/mL cells were sequentially added to the 96-well plate. To achieve better adherence, the 96-well plate was cultured in a dark environment containing 5% CO_2 (37 °C) for 24 h. After that, different materials were configured to different concentrations in the culture medium.

First Group: UCNPs@SP-MA/MAA.

Concentration of nanoparticles (μg/mL)	Duration (Hour)	NIR irradiation (Minute)
6.25, 12.5, 25, 50 and 100	24	0
6.25, 12.5, 25, 50 and 100	24	7

Second Group: DOX-UCNPs@SP-MA/MAA.

Sample	Concentration of DOX (μg/mL)	Duration (Hour)	NIR irradiation (Minute)
DOX-UCNPs@SP-MA/MAA	0.1, 1, 2.5, 5 and 10	24	0
	0.1, 1, 2.5, 5 and 10	24	7

A 0.5 W NIR was used as the light source. MCF-7 cells were placed in a dark environment for 24 h 20 μL of 5 mg/mL MTT solution was then added to each well of a 96-well plate and incubated for 4 h. To avoid the effect of the drug absorption spectrum, to each well, 100 μL of PBS was added to detect the effects of the remaining drug and the particles in solution. Then 150 μL of DMSO was added to each well and shaken at 150 rpm for 15 min. Finally, a microplate reader was used to measure the absorption intensity of the 490 nm wavelength to determine the cell viability in the counting plate.

2.12. Characterization

The size of the nanoparticles was characterized by transmission electron microscopy (TEM) using a Tecnai G20 (FEI Co.) microscope at an acceleration voltage of 200 kV. The emission spectra of the UCNPs were recorded by an Edinburgh FLS980 fluorescence spectrophotometer equipped with a near-infrared (NIR) laser (980 nm, Hi-Tech Optoelectronics Co., Ltd, China) as the excitation source. The absorption spectra were measured by a UV–Vis Spectrophotometer (Hitachi U-3900). The crystal form and type of the core-shell particles were characterized by XRD (a Bruker D8 Advance X-ray powder diffractometer), and the cell survival rate was measured by Microplate reader (ELx800, BioTek, USA).

3. Results and discussion

3.1. Preparation of UCNPs@SP-MA/MAA

Scheme 1 shows the synthetic route of monodispersed UCNP@SP-MA/MAA nanocomposites. The monodispersed $NaYF_4$:Yb^{3+}/Tm^{3+} nanoparticles were firstly prepared by solvothermal synthesis with a spherical particle size range of 23–26 nm, as shown in the TEM images in Fig. 1a. $NaYF_4$:Yb^{3+}/Tm^{3+} was further synthesized into $NaYF_4$:Yb^{3+}/Tm^{3+}@$NaYF_4$ to improve the particle luminescence stability, as shown in Figure S1. The ellipsoid shape of $NaYF_4$:Yb^{3+}/Tm^{3+}@$NaYF_4$ showed a good dispersion with particle sizes of about 42–44 nm (Fig. 1b). In this study, Na+, F- ions (by adding NaOH and NH_4F) were introduced to the reaction system to control the rate of reaction to form amorphous $NaYF_4$ precipitation and the particle size. The original amorphous $NaYF_4$

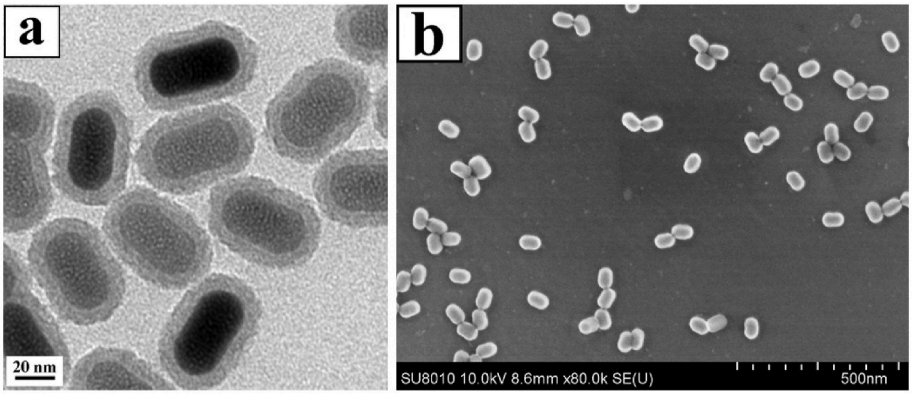

Fig. 2. TEM images of (a) $NaYF_4$: Yb^{3+}/Tm^{3+}@$NaYF_4$@SiO_2. (b) SEM images of $NaYF_4$: Yb^{3+}/Tm^{3+}@$NaYF_4$@SiO_2.

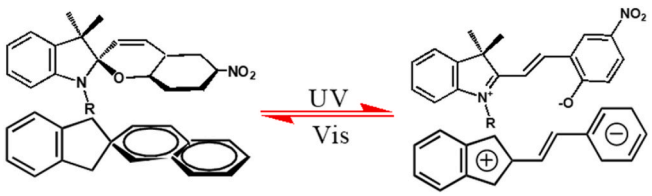

Fig. 3. Schematic diagram of the spiropyran isomerization process under UV and visible light.

precipitates could be crystallized on the surface of the pre-crystallized $NaYF_4$: Yb^{3+}/Tm^{3+} nanoparticles through the solvothermal method. The crystalline structure of the nanoparticles was determined by the XRD technique, as shown in Figure S2. Yb^{3+} acted as a sensitizer to enhance the luminescence efficiency of the up-conversion process. Tm^{3+} acted as an activator due to the strong absorption at 980 nm and its outer electron transition caused upconverting fluorescence which could be used for biological imaging. In Fig. 1a and b, the UCNPs exhibit good dispersibility in an organic solvent by the oleic acid ligand on the surface.

A non-toxic and hydrophilic silica layer can enhance the chemical and light/heat stability and act as a mediator for further spiropyranyl shell coating. A uniform 5–6 nm silica shell was formed on the surface of the nanoparticles by TEOS hydrolysis (Fig. 2a and b). 3-(Trimethoxysilyl) propyl methacrylate (kh-570), as the coupling agent, was introduced to achieve a highly active double bond group on the surface of the particles. The silica shell was used to coat the organic layer and provide a certain physical space for the drug loading in the follow-up study.

To functionalize the UCNPs@SiO_2 particles and further achieve controlled-release of drugs, spiropyran was introduced to modify the UCNPs@SiO_2 particles. From the schematic diagram of the spiropyran isomerization process shown in Fig. 3, the sulfonium ring and the benzospiropyrene in the spiropyran molecule are connected by a snail carbon atom, and the two rings are orthogonal in three-dimensional space. The closed-loop spiropyran molecules are stimulated by UV light (λ = 365 nm)/pH to change the structure. With the snail carbon atom changing from sp3 to sp2 structure, the *C*–O bond breaks and the conformation and electron arrangement of the molecule change, forming a conjugated planar structure. The dipole moment of SP is in the range of B 4–6 D, which drastically changes to B 14–18 D for the MC, leading to a strong absorption peak appearing at 500–600 nm in Figure S3.

The UCNPs@SiO_2@SP-MA/MAA was synthesized through distillation precipitation polymerization with UCNPs@SiO_2 particles as the matrix, MAA and SP-MA as the monomer, and EGDMA as the cross-linker. Figure S4 shows the FTIR spectra of the monomer SP-OH and modified monomer SP-MA. The FTIR spectra of the OA-UCNPs, UCNPs@SiO_2, UCNPs@SiO_2@SP-MA/MAA, and UCNPs@SP-MA/MAA are shown in Figure S5. According to Fig. 4a, the optimal thickness of the poly SP-MA/MAA layer was about 8 ± 0.5 nm with the mole ratio of SP-MA:MAA being kept at 1:0.3. Then, the silica layer was etched by HF to obtain the yolk-shell UCNPs@SP-MA/MAA nanocomposites shown in Fig. 4b. The size of UCNPs@SP-MA/MAA nanocomposites was about 60 ± 0.5 nm. The EDS data of UCNPs@SiO_2@SP-MA/MAA and UCNPs@SP-MA/MAA demonstrated that the SiO_2 layer vanished, as shown in Figure S6.

3.2. *pH responsive behavior of the nanocomposites*

The size changes of the UCNPs@SP-MA/MAA nanocomposites were also studied in different acid-based environments through DLS. In Fig. 5a, with a stable closed-loop structure (SP) at pH 7.4, transforming to an open-loop structure (MCH+) at pH 4.5, the nanocomposites are swollen from 78 nm at pH 7.4–92 nm at pH 4.5. The increase of the

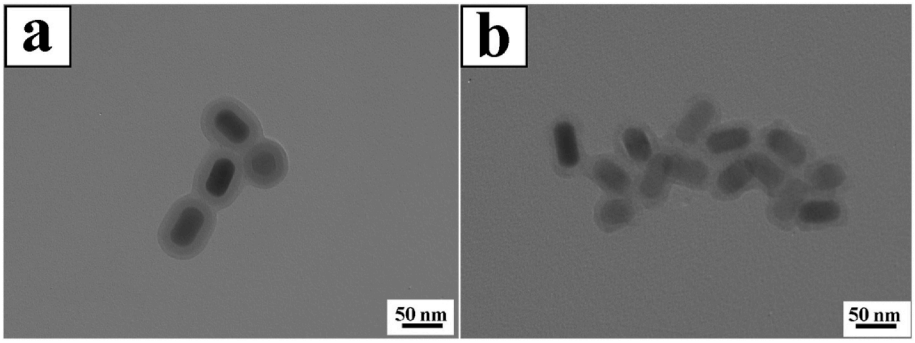

Fig. 4. TEM image of (a) UCNPs@SiO_2@SP-MA/MAA nanoparticles and (b) UCNPs@SP-MA/MAA nanocomposites.

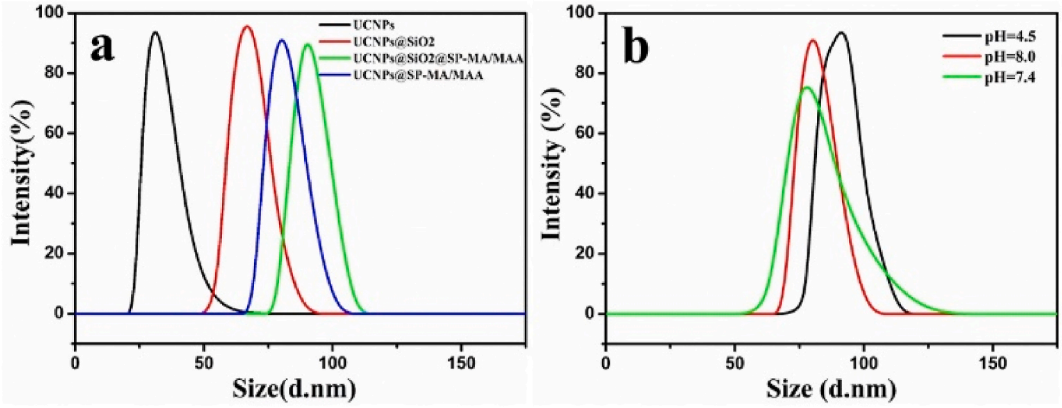

Fig. 5. DLS measurements of particle size variation (a) at each synthetic process and (b) under different pH.

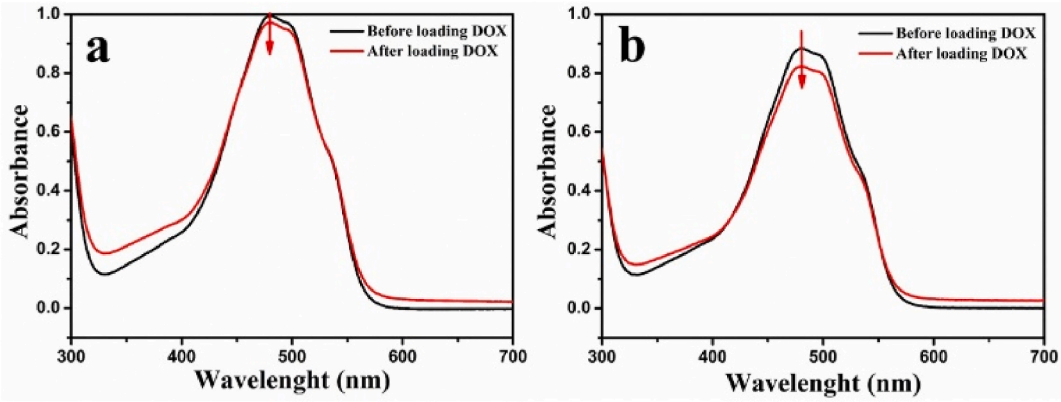

Fig. 6. UV–Vis absorption spectrum of UCNPs@SP-MA/MAA before and after drug loading under different pH (a) 4.5 and (b) 7.4.

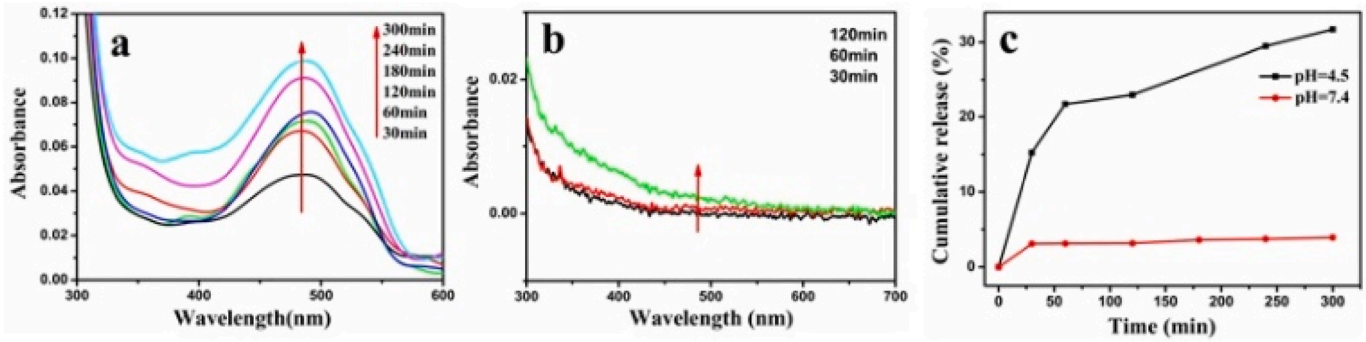

Fig. 7. The absorbance change of released DOX from DOX-UCNPs@SP-MA/MAA under different pH (a) pH 4.5 and (b) pH 7.4, (c) Cumulative release of DOX from UCNPs@SP-MA/MAA nanocomposites as a function of time under pH 4.5 (black line) and pH 7.4 (red line). (For interpretation of the references to color in this figure legend, the reader is referred to the Web version of this article.)

dipole moment was caused by the SP protonation process and the formation of its open-loop structure. At low pH, the SP-type of spiropyran ring was converted into an open-loop MCH + structure, causing electrostatic interaction of the protonated isomer. After deprotonation by washing with buffer solution, the MCH + restored the SP structure, and the particle size returned to 80 nm as illustrated by the red line in Fig. 5b.

3.3. Loading DOX into UCNPs@SP-MA/MAA

DOX as the target drug was used to explore the drug loading and release behavior of the UCNPs@SP-MA/MAA nanoparticles. Fig. 6a and b shows the loading of 1 mg particles at different pH values (4.5, 7.4) at a concentration of 3 mL 0.05 mg/mL DOX solution. With the solution pH value increase, the drug loading efficiency was improved. At pH 4.5, spiropyran existed as MCH + excluding DOX (+2.2 mV), and the protonated NH_2 in DOX also had difficulty in forming hydrogen bonds. Moreover, a swollen shell with decreased shell density is not favorable for drug encapsulation. These three factors (weak hydrogen bonding, electrostatic repulsion, decreased shell density) would result in a decreased drug loading at pH 4.5 (in Fig. 6a). At pH 7.4, the spiropyran existed as SP, which has no repulsive force with DOX anymore. Under neutral conditions, the $–NH_2$- in DOX could exert a positive effect on the hydrogen bonding interactions with spiropyran. Multiple hydrogen bonding ($–NH_2–$, –OH) interaction between them is favorable for drug loading. In Fig. 6b, the amount of drug absorbed reaches 10 *wt*% when 20 mg of UCNPs@SP-MA/MAA is dispersed in 10 mL (1 mg/mL) DOX solution. Fluorescence microscopy images of 40 mg UCNPs@SP-MA/MAA nanocomposites loaded with DOX are shown in Figure S7.

3.4. pH-controlled release behavior of DOX-UCNPs@SP-MA/MAA nanocomposites

Fig. 7 shows the drug controlled-release of UCNPs@SP-MA/MAA nanocomposites at different pH values. At pH 4.5, the SP-type of spiropyran ring was converted into an open-loop MCH + structure. Electrostatic repulsion between the spiropyran (protonated MCH+) caused the size of UCNPs@SP-MA/MAA nanocomposites to decrease with the shell layer density. Furthermore, the spiropyran (protonated MCH+) had a repulsion effect with DOX (Zeta potential: +2.2 mV). Moreover, under pH 4.5, protonated -NH^{3+} in DOX did not exert a positive effect on the hydrogen bonding interactions with the nanocomposites. These three factors (weak hydrogen bonding, electrostatic repulsion, decreased shell density) resulted in 31.7% of release in 300 min at pH 4.5. As shown in Fig. 4b, while at pH 7.4, there was only 3.9% DOX released in 300 min. In the other words, 96.1% DOX was stably encapsulated in the nanocomposites.

It is known that cancer tissue lysosomes have a lower pH (pH 4.5–5.0) than physiological pH 7.4 [30]. Our UCNPs@SP-MA has stable encapsulation behavior at a physiological pH 7.4 and responsive release behavior in cancer tissue lysosomes, which is very important for the cure of tumors. The fluorescence microscopy images show that DOX was released outside the dialysis bag, as shown in Figure S8. Fluorescence only existed in DOX-UCNPs@SP-MA/MAA before release, and fluorescence outside the dialysis bag gradually increased after 24 h.

3.5. NIR responsive property and controlled release behavior of DOX-UCNPs@SP-MA/MAA nanocomposites

The UCL mechanism of $NaYF_4$:Yb^{3+}/Tm^{3+} is shown in Figure S9. The

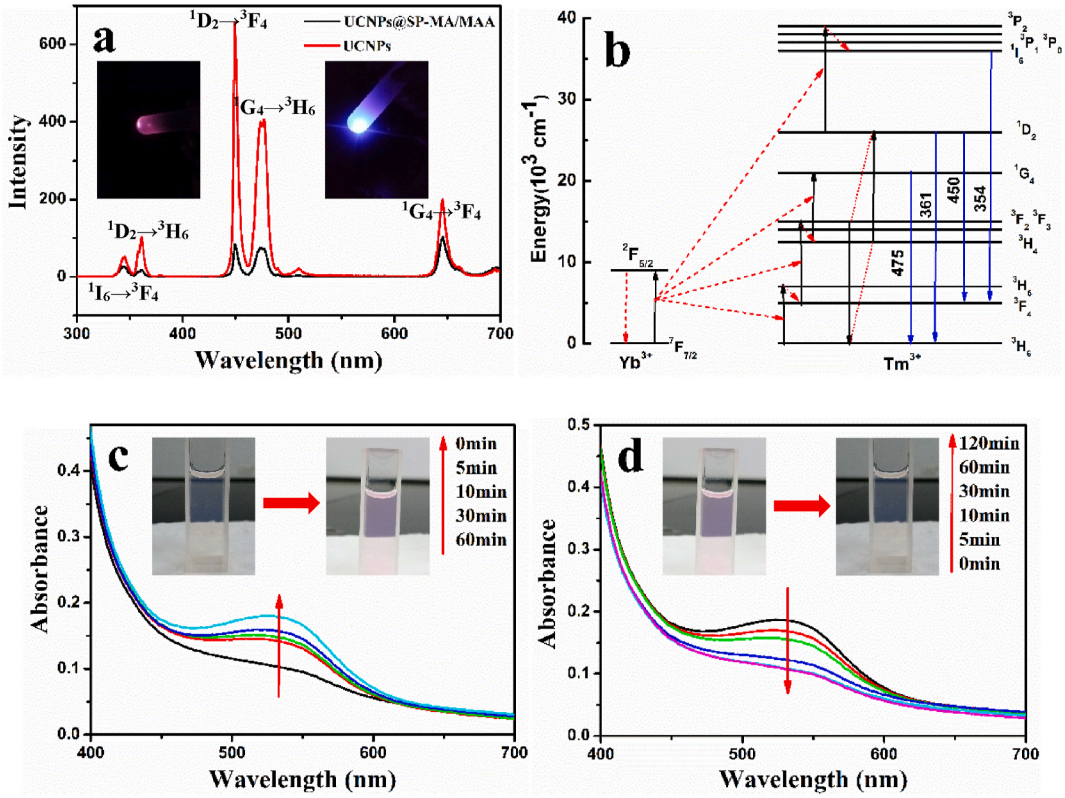

Fig. 8. (a) Up-conversion emission spectrum of $NaYF_4$: Yb^{3+}/Tm^{3+} nanoparticles under 980 nm NIR irradiation. (b) Energy levels and luminescence principle of $NaYF_4$: Yb^{3+}/Tm^{3+} nanoparticles. UV–Vis absorption spectrum of UCNPs@SiO_2@SP-MA/MAA under (c) NIR irradiation and (d) visible light.

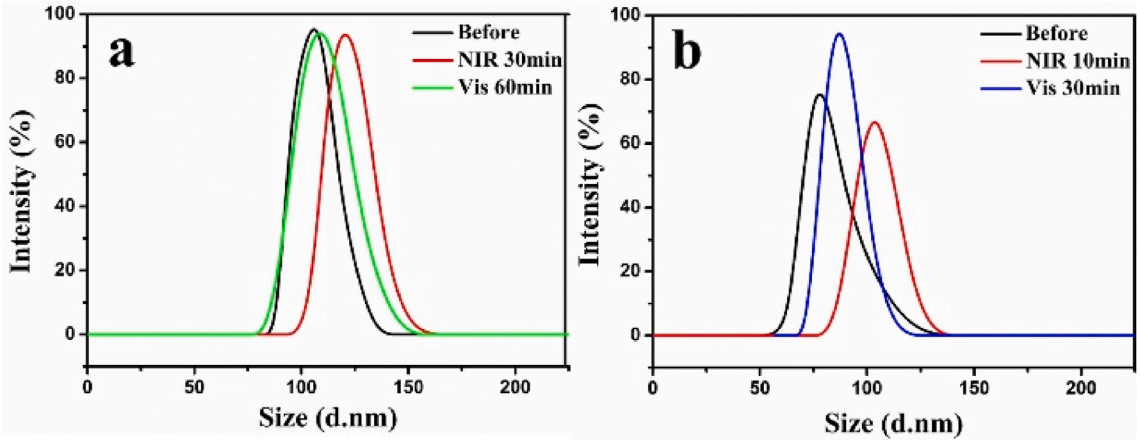

Fig. 9. (a) Hydrodynamic diameters of UCNPs@SiO_2@SP-MA/MAA nanocomposites before and after NIR and visible light irradiation (b) Hydrodynamic diameters of UCNPs@SP-MA/MAA nanocomposites before and after NIR irradiation.

UV to visible emission bands of the UCL spectrum of the Yb^{3+}/Tm^{3+} transition include ~365 nm (1D2-3H6), ~450 nm (1D2-3H4) and ~475 nm (1G4-3H6) in Fig. 8a and b, of which a large part of the emission can be absorbed by the spiropyran group. The simultaneous emission of the core-UCNPs structure in the multilayer structure, both ultraviolet and visible, could achieve reversible photoisomerization of the spiropyran in the shell network.

Fig. 8c and d shows the UV–Vis absorption spectra of UCNPs@SiO_2@SP-MA/MAA under NIR irradiation and visible light. From the UV–Vis absorption spectrum of UCNPs@SiO_2@SP-MA/MAA, it can be observed that the absorption peak of MC at $\lambda = 523$ nm gradually increases under NIR irradiation. After 60-min irradiation, the absorption of the particles reached a stable level with the color change to light-red. The spiryoran shell stimulated by the NIR light can realize the transformation from SP to MC, as shown in Fig. 8, where the absorption peak gradually decreases and vanishes at 120 min with the color being restored colorless. In contrast, the UCNPs@SiO_2 has no obvious absorption peak at $\lambda = 400$–600 nm, as shown in Figure S10. When the SP is converted to the MC isomer, the molecular dipole moment changes from 4.3 D to 17.7 D [16]. With the SP isomer converting to the MC isomer, the dipole moment of the molecule changes, resulting in the hydrophobic shell changing to a hydrophilic shell, which was also confirmed by the water contact angles of UCNPs@SP-MA/MAA in Figure S11. The existence of the hydrophobic shell can protect the drug molecules from the external hydrophilic environment and provide a certain barrier function. After NIR irradiation, the hydrophilic polymer

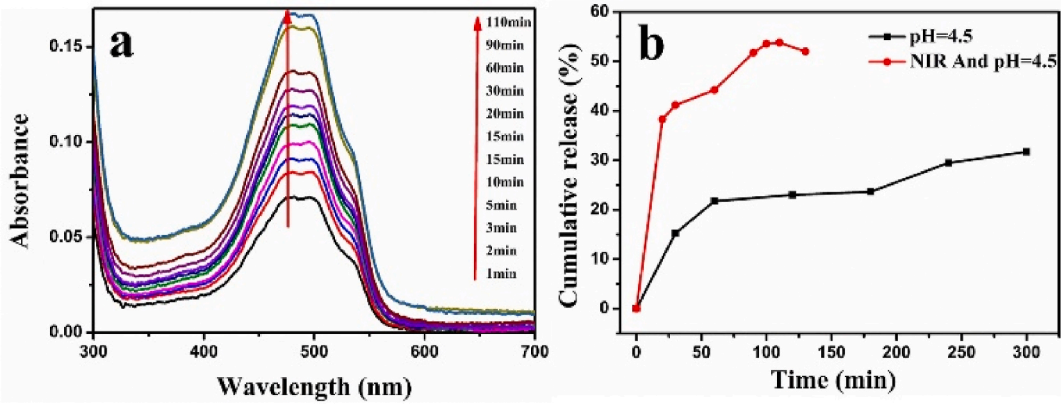

Fig. 10. (a) The UV–Vis absorbance spectrum change of DOX release from DOX-UCNPs@SP-MA/MAA under pH 4.5 and NIR. (b) Cumulative release of DOX from UCNPs@SP-MA/MAA under different conditions: pH 4.5 (black line), pH 4.5 with NIR irradiation (red line). (For interpretation of the references to color in this figure legend, the reader is referred to the Web version of this article.)

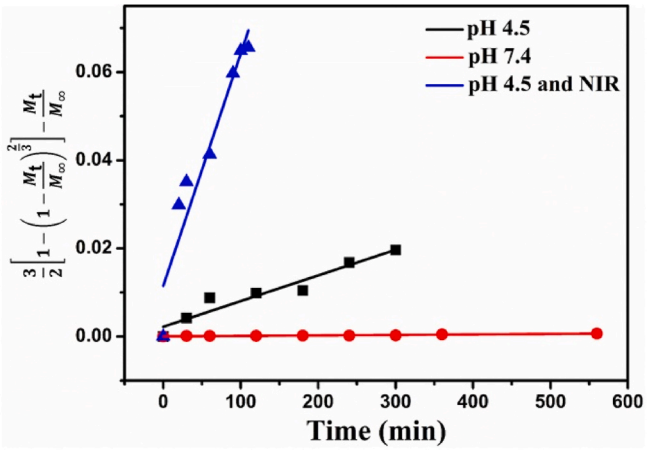

Fig. 11. Linear regression analysis using the Baker–Lonsdale model of the profile of DOX release from UCNPs@SP-MA/MAA nanocomposites as a function of time under different conditions.

shell can achieve selective penetration of hydrophilic drugs, which is beneficial for drug release.

In Fig. 9a, the average particle size of UCNPs@SiO_2@SP-MA/MAA nanocomposites in dark conditions was 105 nm, while the particle size increased to 120 nm after 30 min of NIR irradiation. The particle size returned to 108 nm after continuous exposure to visible light for 60 min. To further verify the change process of the particle size response of UCNPs@SP-MA/MAA under different light conditions, UCNPs@-SiO_2@SP-MA/MAA was etched to obtain UCNPs@SP-MA/MAA nanocomposites. The size of UCNPs@SP-MA/MAA nanocapsulte decreased from 105 nm to 78 nm, shrinking after HF etching. Under NIR irradiation for 10 min, the size of UCNPs@SP-MA/MAA nanocomposites changed from 78 nm to 99 nm, in which hydrophobic SP was transformed to hydrophilic MC leading to the polymeric layer swelling, as shown in Fig. 5b.

Fig. 10 shows the release curves of the combined effect of NIR light and pH 4.5. On the one hand, the SP isomer transformed to MC isomer by NIR irradiation with increased shell size, and on the other hand, spiropyran directly changed from SP to protonated MCH + type under acidic conditions. The increased shell size and the electrostatic repulsion between the drugs and polymers enhanced the DOX release from the DOX-UCNPs@SP-MA/MAA nanocomposites. Under the continuous synergy of pH and NIR light reaction, the cumulative release of the drug reached a maximum value of about 53.8% after 110 min, as shown in Fig. 10b.

Various models have been used to describe the release of drugs from different matrices. In our work, the commonly used Baker–Lonsdale model for spherical matrix was applied to quantify the release of DOX-UCNPs@SP-MA/MAA nanocomposites under different conditions [43–45], as described below.

$$\frac{3}{2}\left[1-\left(1-\frac{M_t}{M_\infty}\right)^{\frac{2}{3}}\right]-\frac{M_t}{M_\infty}=\frac{3DC_s}{r_0^2C_0}\cdot t$$

where Mt and M_∞ represent the amount of DOX at time t and t = ∞, respectively; the ratio of Mt/M_∞ is the cumulative release of DOX; D is the diffusion coefficient of the DOX from the system; r_0 is the radius of the nanoparticles; C_s is the solubility of the DOX in the system, and C_0 is the original concentration of DOX. The results shown in Fig. 11 indicate that the Baker–Lonsdale model fits for the release profile of DOX under different pHs and NIR illuminations, with the release rate constants ($3DCs/r_0^2C_0$) and the correlation coefficients R^2 5.82 × $10^{-5}$and 0.95 (pH 4.5), 1.07 × $10^{-6}$and 0.96 (pH 7.4, visible light) 5.26 × 10^{-4} and 0.96 (pH: 4.5, NIR light), under independent NIR light and pH controlled release. In the DOX-UCNPs@SP-MA/MAA nanocomposite system, C_0 is equal to C_s, and the diffusion factor D under NIR irradiation and pH 4.5 is one order of magnitude greater than the diffusion factor D under pH 4.5, indicating that the largest release rate can be realized under the synergistic effect of NIR and the acidic condition.

The introduction of NIR light further enhanced the drug release effect, and the particle release amount further increased to 53.8% within 110 min under NIR light irradiation and pH = 4.5. There are similar reports about the largest release amount under a combination of light illumination and acidic conditions. Chen and co-workers [40] reported self-assembled nanoparticles constructed of spiropyran-based amphiphilic copolymer with light, pH, and thermo-responsive behavior. The largest drug release amount was achieved under the combination of the UV light stimulation and acidic conditions due to the hydrophilicity further increasing. Wang's group [2] fabricated UCNPs@polymer nanocomposites through the self-assembly of the amphiphilic photo-responsive polymers and the encapsulation of the UCNPs in the core of the self-assemblies, and demonstrated a controlled release triggered by the near-infrared light and pH 5.0. Our work here has successfully demonstrated a core-shell structured drug delivery system with pH and NIR responsive characteristics, which has the ability of intracellular pH-response release and exogenous NIR modulated release.

3.6. Cytotoxicity studies of UCNPs@SP-MA/MAA, DOX-UCNPs@SP-MA/MAA with and without NIR

Investigation of particle cytotoxicity is essential to biological

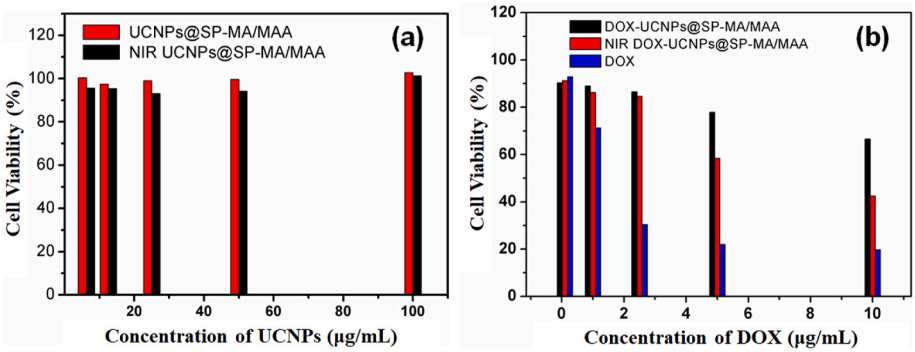

Fig. 12. (a) Cytotoxicity studies of UCNPs@SP-MA/MAA nanoparticles under different conditions: (1) dark conditions (red line) (2) NIR irradiation (black line). (b) cell survival rates under different conditions: DOX-UCNPs@SP-MA/MAA particles (black line), DOX-UCNPs@SP-MA/MAA with NIR light irradiation (red line) and pure drug DOX (blue line). (For interpretation of the references to color in this figure legend, the reader is referred to the Web version of this article.)

applications. In this study, the cell viability of UCNPs@SP-MA/MAA and DOX-UCNPs@SP-MA/MAA was investigated. Fig. 12a shows that different concentrations of the unloaded drug UCNPs@SP-MA/MAA particles with MCF-7 cell survival under two different light conditions: (1) dark conditions (red line) and (2) NIR irradiation (black line). It had no obvious effect on cell viability under low power (0.5 W laser) 980 nm NIR irradiation. This result indicates that both the UCNPs@SP-MA/MAA particles and NIR light have no obvious cytotoxicity. Fig. 12b shows the MCF-7 cell viability under pure DOX (blue line), DOX-loaded UCNPs@SP-MA/MAA particles (black line), and DOX-loaded UCNPs@SP-MA/MAA particles with NIR irradiation (red line). For the cancer cells in presence of pure DOX, it can be found that MCF-7 cells apparently died and the cell survival rate was 71% ± 2% when the concentration of DOX increased to 5 μg/mL. When DOX-loaded UCNPs@SP-MA/MAA particles were cultured with MCF-7 cells (without NIR irradiation) for 24 h, the cell survival rate was higher than the DOX, indicating no significant deaths when the concentration of DOX-loaded UCNPs@SP-MA/MAA particles was 1 μg/mL. When the DOX concentrations in the drug-loaded particles were 1 μg/mL and 10 μg/mL, the cell viabilities were 86.5% and 65.0% respectively. With the increase in concentration of DOX-loaded nanoparticles, cell viability decreased [46–48].

DOX-UCNPs@SP-MA/MAA nanocomposites were cultured with MCF-7 cells for 24 h under NIR irradiation, as shown in Fig. 12b. The survival rates of the cells were only 58% and 42% when the DOX concentration in the drug-loaded particles were 5 μg/mL and 10 μg/mL, respectively. Compared with the non-irradiated group, the significantly reduced cell survival rate indicated that the DOX-UCNPs@SP-MA/MAA nanocomposites under NIR illumination are more effective in killing cells by promoting the release of DOX from DOX-loaded nanoparticles to the cells, which is consistent with the release situation *in vitro*. This work successfully demonstrates a drug delivery system with pH- and NIR controlled encapsulation and release properties, which has enormous potential for improving drug efficacy and preventing undesirable side effects in normal tissues.

4. Conclusions

In this work, UCNP achieved surface modification and multilayer structure design by the distillation precipitation polymerization and template method. Upon NIR light irradiation, the up-conversion fluorescence induced the spiropyran to be isomerized to the merocyanine, which caused the polymer layer to be transformed from hydrophobic to hydrophilic, with particle sizes changing from 78 nm to 99 nm. At pH 4.5, the hydrophobic spiropyran could be also protonated to hydrophilic merocyanine and the polymer shell was swollen from 78 nm to 92 nm. At pH 7.4, spiropyran exists as SP, and the amount of drug loading reached 10 wt%. The cumulative drug release of DOX-UCNPs@SP-MA/MAA reached 53.8% under pH 4.5/NIR light irradiation. In addition, the cytotoxicity of the nanocomposites loaded with anticancer drug DOX on MCF-7 cancer cells indicated that the loaded drugs could kill the cells effectively and the efficiency could be enhanced significantly with NIR light irradiation. The weakly acidic environment of the cancer cells and NIR light stimulated the drug release from the nanocomposites, effectively killing breast cancer cells. The particles achieved a better pH/NIR response in releasing DOX, thus provided a new pathway for the treatment of cancer.

Author statement

Xiaotao Wang: Conceptualization, Methodology, Formal analysis, Supervision, Funding acquisition. Xiaoping Liu: Writing – original draft, Investigation, Methodology. Hongda Zhu: Investigation. Gaowen Zhang: Investigation. Xuefeng Li: Writing – review & editing. Chak-Yin Tang: Validation, Writing – review & editing. Wing-Cheung Law: Formal analysis, Writing – review & editing, Funding acquisition. Xin Zhao: Writing – review & editing.

Declaration of competing interest

The authors declare that they have no known competing financial interests or personal relationships that could have appeared to influence the work reported in this paper.

Acknowledgments

This work was supported by the Natural National Science Foundation of China (51303049 and 31871442), Key Projects of Hubei Provincial Department of Education (D20191404), the Research Grants Council of the Hong Kong Special Administrative Region, China (15202119) and the intra-faculty fund (1-ZVPC) from the Hong Kong Polytechnic University. Appreciations are also given to the Hubei University of Technology for their help with the DSC, UV and FTIR measurements.

Appendix A. Supplementary data

Supplementary data to this article can be found online at https://doi.org/10.1016/j.polymertesting.2020.107042.

References

[1] J.-F. Gohy, Y. Zhao, Photo-responsive block copolymer micelles: design and behavior, Chem. Soc. Rev. 42 (17) (2013) 7117–7129.
[2] X. Wang, C. Liu, Z. Li, C.-Y. Tang, W.-C. Law, X. Gong, Z. Liu, Y. Liao, G. Zhang, S. Long, L. Chen, Thermal and photo dual-responsive core–shell polymeric nanocarriers with encapsulation of upconversion nanoparticles for controlled anticancer drug release, J. Phys. Chem. C 123 (16) (2019) 10658–10665.

[3] R. Jankaew, N. Rodkate, S. Lamlertthon, B. Rutnakornpituk, U. Wichai, G. Ross, M. Rutnakornpituk, "Smart" carboxymethylchitosan hydrogels crosslinked with poly(N-isopropylacrylamide) and poly(acrylic acid) for controlled drug release, Polym. Test. 42 (2015) 26–36.

[4] S. Cichosz, A. Masek, M. Zaborski, Polymer-based sensors: a review, Polym. Test. 67 (2018) 342–348.

[5] C. Ding, Y. Liu, T. Wang, J. Fu, Triple-stimuli-responsive nanocontainers assembled by water-soluble pillar[5]arene-based pseudorotaxanes for controlled release, J. Mater. Chem. B 4 (16) (2016) 2819–2827.

[6] M. Zhou, X. Du, W. Li, X. Li, H. Huang, Q. Liao, B. Shi, X. Zhang, M. Zhang, One-pot synthesis of redox-triggered biodegradable hybrid nanocomposites with a disulfide-bridged silsesquioxane framework for promising drug delivery, J. Mater. Chem. B 5 (23) (2017) 4455–4469.

[7] F. Vischio, E. Fanizza, V. De Bellis, T. Sibillano, C. Ingrosso, C. Giannini, V. Laquintana, N. Denora, A. Agostiano, M. Striccoli, M.L. Curri, N. Depalo, Near-infrared absorbing solid lipid nanoparticles encapsulating plasmonic copper sulfide nanocrystals, J. Phys. Chem. C 123 (37) (2019) 23205–23213.

[8] K.M. Rao, A. Kumar, S.S. Han, Poly(acrylamidoglycolic acid) nanocomposite hydrogels reinforced with cellulose nanocrystals for pH-sensitive controlled release of diclofenac sodium, Polym. Test. 64 (2017) 175–182.

[9] O. Bertrand, C.-A. Fustin, J.-F. Gohy, Multiresponsive micellar systems from photocleavable block copolymers, ACS Macro Lett. 1 (8) (2012) 949–953.

[10] G. Biswas, B.C. Jena, S. Maiti, P. Samanta, M. Mandal, D. Dhara, Photoresponsive block copolymer prodrug nanoparticles as delivery vehicle for single and dual anticancer drugs, ACS Omega 2 (10) (2017) 6677–6690.

[11] P. Mena-Giraldo, S. Pérez-Buitrago, M. Londoño-Berrío, I.C. Ortiz-Trujillo, L. M. Hoyos-Palacio, J. Orozco, Photosensitive nanocarriers for specific delivery of cargo into cells, Sci. Rep. 10 (1) (2020) 2110.

[12] J. Jiang, X. Tong, Y. Zhao, A new design for light-breakable polymer micelles, J. Am. Chem. Soc. 127 (23) (2005) 8290–8291.

[13] S. Shrivastava, H. Matsuoka, Photocleavable amphiphilic diblock copolymer micelles bearing a nitrobenzene block, Colloid Polym. Sci. 294 (5) (2016) 879–887.

[14] J. Henzl, M. Mehlhorn, H. Gawronski, K.H. Rieder, K. Morgenstern, Reversible cis-trans isomerization of a single azobenzene molecule, Angew Chem. Int. Ed. Engl. 45 (4) (2006) 603–606.

[15] H.M. Bandara, S.C. Burdette, Photoisomerization in different classes of azobenzene, Chem. Soc. Rev. 41 (5) (2012) 1809–1825.

[16] R. Klajn, Spiropyran-based dynamic materials, Chem. Soc. Rev. 43 (1) (2014) 148–184.

[17] T. Kudernac, S.J. van der Molen, B.J. van Wees, B.L. Feringa, Uni- and bi-directional light-induced switching of diarylethenes on gold nanoparticles, Chem Commun (Camb) 34 (2006) 3597–3599.

[18] A. Abdollahi, H. Roghani-Mamaqani, B. Razavi, M. Salami-Kalajahi, The light-controlling of temperature-responsivity in stimuli-responsive polymers, Polym. Chem. 10 (42) (2019) 5686–5720.

[19] W. Fuß, C. Kosmidis, W.E. Schmid, S.A. Trushin, The photochemical cis–trans isomerization of free stilbene molecules follows a hula-twist pathway, Angew. Chem. Int. Ed. 43 (32) (2004) 4178–4182.

[20] J. Zhang, J.K. Whitesell, M.A. Fox, Photoreactivity of self-assembled monolayers of azobenzene or stilbene derivatives capped on colloidal gold clusters, Chem. Mater. 13 (7) (2001) 2323–2331.

[21] Q. Jin, G. Liu, J. Ji, Micelles and reverse micelles with a photo and thermo double-responsive block copolymer, J. Polym. Sci. Polym. Chem. 48 (13) (2010) 2855–2861.

[22] D.A. Davis, A. Hamilton, J. Yang, L.D. Cremar, D. Van Gough, S.L. Potisek, M. T. Ong, P.V. Braun, T.J. Martinez, S.R. White, J.S. Moore, N.R. Sottos, Force-induced activation of covalent bonds in mechanoresponsive polymeric materials, Nature 459 (7243) (2009) 68–72.

[23] Y. Zhao, Light-responsive block copolymer micelles, Macromolecules 45 (9) (2012) 3647–3657.

[24] X. Wang, J. Hu, G. Liu, J. Tian, H. Wang, M. Gong, S. Liu, Reversibly switching bilayer permeability and release modules of photochromic polymersomes stabilized by cooperative noncovalent interactions, J. Am. Chem. Soc. 137 (48) (2015) 15262–15275.

[25] S. Chen, F. Jiang, Z. Cao, G. Wang, Z.-M. Dang, Photo, pH, and thermo triple-responsive spiropyran-based copolymer nanoparticles for controlled release, Chem. Commun. 51 (63) (2015) 12633–12636.

[26] V.K. Kotharangannagari, A. Sánchez-Ferrer, J. Ruokolainen, R. Mezzenga, Photoresponsive reversible aggregation and dissolution of rod–coil polypeptide diblock copolymers, Macromolecules 44 (12) (2011) 4569–4573.

[27] J.N. Liu, W.B. Bu, J.L. Shi, Silica coated upconversion nanoparticles: a versatile platform for the development of efficient theranostics, Acc. Chem. Res. 48 (7) (2015) 1797–1805.

[28] J. Zhou, Q. Liu, W. Feng, Y. Sun, F. Li, Upconversion luminescent materials: advances and applications, Chem. Rev. 115 (1) (2015) 395–465.

[29] X. Liu, R. Deng, Y. Zhang, Y. Wang, H. Chang, L. Huang, X. Liu, Probing the nature of upconversion nanocrystals: instrumentation matters, Chem. Soc. Rev. 44 (6) (2015) 1479–1508.

[30] N.M. Idris, M.K.G. Jayakumar, A. Bansal, Y. Zhang, Upconversion nanoparticles as versatile light nanotransducers for photoactivation applications, Chem. Soc. Rev. 44 (6) (2015) 1449–1478.

[31] Y. Huang, E. Hemmer, F. Rosei, F. Vetrone, Multifunctional liposome nanocarriers combining upconverting nanoparticles and anticancer drugs, J. Phys. Chem. B 120 (22) (2016) 4992–5001.

[32] Y. Huang, F. Rosei, F. Vetrone, A single multifunctional nanoplatform based on upconversion luminescence and gold nanorods, Nanoscale 7 (12) (2015) 5178–5185.

[33] X. Michalet, F.F. Pinaud, L.A. Bentolila, J.M. Tsay, S. Doose, J.J. Li, G. Sundaresan, A.M. Wu, S.S. Gambhir, S. Weiss, Quantum dots for live cells, in vivo imaging, and diagnostics, Science 307 (5709) (2005) 538–544.

[34] X. Kang, Z. Cheng, C. Li, D. Yang, M. Shang, P.a. Ma, G. Li, N. Liu, J. Lin, Core–shell structured up-conversion luminescent and mesoporous NaYF4:Yb3+/Er3+ @nSiO2@mSiO2 nanospheres as carriers for drug delivery, J. Phys. Chem. C 115 (32) (2011) 15801–15811.

[35] Y. Yang, F. Liu, X. Liu, B. Xing, NIR light controlled photorelease of siRNA and its targeted intracellular delivery based on upconversion nanoparticles, Nanoscale 5 (1) (2013) 231–238.

[36] G. Chen, T.Y. Ohulchanskyy, S. Liu, W.-C. Law, F. Wu, M.T. Swihart, H. Ågren, P. N. Prasad, Core/shell $NaGdF_4$:Nd^{3+}/$NaGdF_4$ nanocrystals with efficient near-infrared to near-infrared downconversion photoluminescence for bioimaging applications, ACS Nano 6 (4) (2012) 2969–2977.

[37] F. Wang, X. Liu, Recent advances in the chemistry of lanthanide-doped upconversion nanocrystals, Chem. Soc. Rev. 38 (4) (2009) 976–989.

[38] J.F. Suyver, A. Aebischer, D. Biner, P. Gerner, J. Grimm, S. Heer, K.W. Krämer, C. Reinhard, H.U. Güdel, Novel materials doped with trivalent lanthanides and transition metal ions showing near-infrared to visible photon upconversion, Opt. Mater. 27 (6) (2005) 1111–1130.

[39] C. Liu, Y. Zhang, M. Liu, Z. Chen, Y. Lin, W. Li, F. Cao, Z. Liu, J. Ren, X. Qu, A NIR-controlled cage mimicking system for hydrophobic drug mediated cancer therapy, Biomaterials 139 (2017) 151–162.

[40] S. Chen, Y. Gao, Z. Cao, B. Wu, L. Wang, H. Wang, Z. Dang, G. Wang, Nanocomposites of spiropyran-functionalized polymers and upconversion nanoparticles for controlled release stimulated by near-infrared light and pH, Macromolecules 49 (19) (2016) 7490–7496.

[41] F. Bai, X. Yang, W. Huang, Preparation of narrow or monodisperse poly (ethyleneglycol dimethacrylate) microspheres by distillation–precipitation polymerization, Eur. Polym. J. 42 (9) (2006) 2088–2097.

[42] D.S. Achilleos, T.A. Hatton, M. Vamvakaki, Light-regulated supramolecular engineering of polymeric nanocomposites, J. Am. Chem. Soc. 134 (13) (2012) 5726–5729.

[43] S. Radin, T. Chen, P. Ducheyne, The controlled release of drugs from emulsified, sol gel processed silica microspheres, Biomaterials 30 (5) (2009) 850–858.

[44] J.O. Kim, A.V. Kabanov, T.K. Bronich, Polymer micelles with cross-linked polyanion core for delivery of a cationic drug doxorubicin, J. Contr. Release 138 (3) (2009) 197–204.

[45] H. Hu, H. Wang, Q. Du, Preparation of pH-sensitive polyacrylic acid hollow microspheres and their release properties, Soft Matter 8 (25) (2012) 6816–6822.

[46] C. Wang, L. Cheng, Y. Liu, X. Wang, X. Ma, Z. Deng, Y. Li, Z. Liu, Imaging-guided pH-sensitive photodynamic therapy using charge reversible upconversion nanoparticles under near-infrared light, Adv. Funct. Mater. 23 (24) (2013) 3077–3086.

[47] F. Muhammad, M. Guo, W. Qi, F. Sun, A. Wang, Y. Guo, G. Zhu, pH-Triggered controlled drug release from mesoporous silica nanoparticles via intracelluar dissolution of ZnO nanolids, J. Am. Chem. Soc. 133 (23) (2011) 8778–8781.

[48] G. Wang, J. Dong, T. Yuan, J. Zhang, L. Wang, H. Wang, Visible light and pH responsive polymer-coated mesoporous silica nanohybrids for controlled release, Macromol. Biosci. 16 (7) (2016) 990–994.